# Bay K 8644 Reveals Two Components of L-Type $Ca^{2+}$ Channel Current in Clonal Rat Pituitary Cells

DANIEL M. FASS* and EDWIN S. LEVITAN*‡

From the Departments of *Neuroscience and ‡Pharmacology, University of Pittsburgh, Pittsburgh, Pennsylvania 15261

ABSTRACT Whole-cell L-type $Ca^{2+}$ channel current was recorded in $GH_3$ clonal rat pituitary cells using $Ba^{2+}$ as a charge carrier. In the presence of the dihydropyridine agonist Bay K 8644, deactivation was best described by two exponential components with time constants of ~2 and ~8 ms when recorded at −40 mV. The slow component activated at more negative potentials than the fast component: Half-maximal activation for the slow and fast components occurred at ~−15 and ~1 mV, respectively. The fast component was more sensitive to enhancement by racemic Bay K 8644 than the slow component: $ED_{50fast}$ = ~21 nM, $ED_{50slow}$ = ~74 nM. Thyrotropin-releasing hormone (TRH; 1 μM) inhibited the slow component by ~46%, whereas the fast component was inhibited by ~22%. TRH inhibition of total L-current showed some voltage dependence, but each Bay K 8644–revealed component of L-current was inhibited in a voltage-independent manner. Therefore, the apparent voltage dependence of TRH action is derived from complexities in channel gating rather than from relief of inhibition at high voltages. In summary, Bay K 8644–enhanced L-currents in $GH_3$ cells consist of two components with different sensitivities to voltage, racemic Bay K 8644, and the neuropeptide TRH. Key words: calcium channel • dihydropyridine • thyrotropin-releasing hormone • $GH_3$

## INTRODUCTION

Biophysical and pharmacological measurements have revealed the existence of multiple components of $Ca^{2+}$ current in virtually every type of excitable cell studied (Bean, 1989*a*; Hess, 1990). The $Ca^{2+}$ current components identified by these methods differ in their sensitivities to specific drugs and toxins, single-channel conductances, and voltage dependences. For example, L-type $Ca^{2+}$ channels are sensitive to dihydropyridines (DHP),[1] have a large single-channel conductance, and are activated by relatively high levels of depolarization.

Within most classes of $Ca^{2+}$ current, heterogeneity is evident. For example, there are differences in the kinetic properties of L-currents in different cell types. L-currents activate rapidly in cardiac cells but slowly in skeletal muscle cells (Tanabe et al., 1991). In general, L-currents inactivate more rapidly in cardiac cells than in neurons (see Hess, 1990). In addition, numerous studies have found distinct multiple components of L-current in an individual cell. These components have been found to differ in their kinetic properties (Cognard et al., 1986; Richard et al., 1990), single-channel conductances (Worley et al., 1986), and DHP sensitivities (Richard et al., 1990; Neveu et al., 1993; Tiaho et al., 1994). Thus, it appears that $Ca^{2+}$ currents designated as L-type comprise a heterogenous family.

In some cells, it is possible to differentiate among $Ca^{2+}$ current classes based on the effects of modulators. For example, in $GH_3$ cells, thyrotropin-releasing hormone (TRH) acts by mobilizing intracellular calcium to inhibit L-currents, but not T-currents (Kramer et al., 1991). In some cases, it is even possible to distinguish selective effects of modulators on individual components of a given class of $Ca^{2+}$ current. For example, isoprenaline preferentially enhances one component of macroscopic L-current in rat ventricular myocytes (Richard et al., 1990; Tiaho et al., 1994) and rat aortic myocytes (Neveu et al., 1994). On the single-channel level, several transmitters have effects that are specific to individual gating modes. For example, norepinephrine inhibits one mode and increases another mode of N-type $Ca^{2+}$ channel gating in frog sympathetic neurons (Delcour and Tsien, 1993). Similar mode-specific effects have been found for isoproterenol modulation of L-channels in guinea pig ventricular myocytes (Yue et al., 1990). Thus, sensitivity to modulation may be an important defining characteristic for each component of $Ca^{2+}$ current.

We have studied $Ca^{2+}$ currents in $GH_3$ rat anterior pituitary tumor cells. High voltage–activated $Ca^{2+}$ current in these cells is relatively easily isolated and is thought to be entirely L-current (Simasko et al., 1988; Kramer et al., 1991; Lievano et al., 1994). In this paper we demonstrate that, in the presence of the DHP agonist Bay K 8644, two components of whole-cell $Ba^{2+}$ current are present. These two components differ in deactivation kinetics, voltage dependence of activation, and sensitivity to the DHP agonist Bay K 8644. In addition, we find

Address correspondence to Edwin S. Levitan, E1355 Biomedical Science Tower, Department of Pharmacology, University of Pittsburgh, Pittsburgh, PA 15261. Fax: (412) 648-1945; E-mail: Levitan@bns.pitt.edu

[1]*Abbreviations used in this paper:* DHP, dihydropyridine; *G–V*, conductance–voltage; TRH, thyrotropin-releasing hormone.


J. GEN. PHYSIOL. © The Rockefeller University Press • 0022-1295/96/07/01/11 $2.00
Volume 108 July 1996 1–11

that TRH preferentially inhibits one of the two L-current components in $GH_3$ cells. Furthermore, we show that TRH inhibition appears to be voltage dependent when total L-current is analyzed but is voltage independent when L-current components are analyzed separately. The distinct properties of the two components suggest that they may participate differentially in cellular processes initiated by $Ca^{2+}$ influx.

## MATERIALS AND METHODS

### *Cell Culture*

$GH_3$ cells were obtained from the American Type Culture Collection (Rockville, MD). The cells were grown at 37°C and 5% $CO_2$ in Ham's F-10 medium supplemented with 15% horse serum and 2.5% fetal calf serum. After passage, cells were plated in 35-mm culture dishes in the same medium and serum but with the addition of either of two media supplements (GMS-S or Ultroser HY; GIBCO BRL, Gaithersburg, MD) that sometimes improved the frequency of seal formation. Use of these media supplements did not alter L-channel properties. Cells were used for electrophysiological experiments 1 to 6 d after passage.

### *Patch-Clamp Experiments*

For all experiments, standard whole-cell patch-clamp methodology was used (Hamill et al., 1981). To begin an experiment, a dish of cells was removed from the incubator, and the incubation medium was aspirated and replaced with the bath solution (150 mM NaCl, 0.8 mM $MgCl_2$, 5.4 mM KCl, 2 mM $CaCl_2 \cdot 2H_2O$, 20 mM glucose, 10 mM Na-HEPES, pH 7.4). After establishment of the whole-cell configuration, the extracellular solution (100 mM $BaCl_2$, 20 mM tetraethylammonium chloride, 10 mM Na-HEPES, pH 7.4) was superfused directly over the cell being studied. Superfusion was maintained continuously throughout all experiments. Pipettes were filled with the pipette solution (160 mM CsCl, 5 mM $MgCl_2$, 0.1 mM EGTA, 0.2 mM NaGTP, 2.5 mM $Na_2$-ATP, 5 mM Cs-HEPES, pH 7.2 with NaOH). All solutions were filtered through 0.2-μm syringe filters (Gelman Sciences, Inc., Ann Arbor, MI). In experiments in which the continuous presence of Bay K 8644 was desired, both the pipette solution and the extracellular solution contained 1 μM of drug.

For experiments performed in the presence of Bay K 8644, pipettes of 1.5–2.0 MΩ tip resistance were fabricated from Kimax-51 glass capillary tubes and coated with Sylgard (Dow Corning Corp., Indianapolis, IN). On average, series resistance was 2.75 MΩ after establishment of the whole-cell configuration and was always compensated by ≥80%. Analog current signals were filtered at 10 kHz and then digitized at 20 kHz. All traces have been leak subtracted by addition of one or two scaled current traces produced by a 40-mV hyperpolarizing pulse given from the holding potential of −40 mV. All data acquisition and curve fitting of raw data were performed using an EPC9 patch-clamp system (HEKA, Lambrecht, Germany). All experiments were performed at room temperature (20–22°C). For experiments performed in the absence of Bay K 8644 ($n$ = 4; see open circles in Fig. 6 *B*), the above protocols were used with the following exceptions: Series resistance averaged 3.25 MΩ, series resistance compensation varied from 0 to 50%, and analog current signals were filtered at 6 kHz and then digitized at 50 kHz.

In the figures, some current traces have been digitally filtered (2–5 kHz) for presentation.

### *Curve-fitting Procedures and Statistics*

Exponential curve fitting of tail currents was performed using the Review program from the software package provided with the EPC-9 patch clamp system. This program uses a simplex algorithm to determine least-squares fits of exponentials to data. The first ~300 μs of the tail currents was ignored in the fitting procedure to avoid artifacts produced by the settling of the voltage clamp. However, amplitude values reflect the extrapolation of the fit back to the time of repolarization. For all fits, initial τ values were set at 2 and/or 8 ms based on results from pilot studies, and amplitude values were set by eye. All parameters ($Amplitude_{fast}$, $Amplitude_{slow}$, $\tau_{fast}$, $\tau_{slow}$, and baseline) were then free to vary. Iterative fits were continued until values ceased changing by >0.1%.

A statistical test that compared the quality of fits of tail currents by single vs double exponentials was performed using the data analysis program PRISM (GraphPAD Software for Science, San Diego, CA). The test involved calculating an F-statistic that evaluates whether the reduction in the sum-of-squares of the residuals from the double-exponential fit (relative to the single-exponential fit) justifies the use of more free parameters; the double exponential has five free parameters ($Amplitude_{fast}$, $Amplitude_{slow}$, $\tau_{fast}$, $\tau_{slow}$, and baseline), whereas the single exponential has three (Amplitude, τ, and baseline).

Nonlinear regression curve fitting of conductance–voltage ($G$–$V$) relations (see Figs. 1, 4, and 9) and dose–response relations (see Fig. 5) were also performed using PRISM. For nonlinear regression, this program uses the Marquardt method for minimizing the sum-of-squares of the residuals. $G$–$V$ relations were fit to Boltzmann equations in the form:

$$G = MAX/(1 + e^{[(V50 - V)/SLOPE]}),$$

where *MAX* was maximum conductance value, *V50* was the half-maximal activation voltage, and *SLOPE* represents the steepness of the voltage dependence. *MAX*, *V50*, and *SLOPE* were free to vary. Normalized dose–response relations were fit to a single-site, sigmoidal equation of the form:

$$\text{RESPONSE} = 100/\{1 + (EC_{50}/[\text{Bay K 8644}])\},$$

where $EC_{50}$ was the half-maximal response dose of Bay K 8644. $EC_{50}$ was free to vary.

A linear regression fit (see Fig. 8 *B*) was also performed using PRISM. In addition to reporting an $r^2$ value for the fit, PRISM assesses whether the slope is significantly different from zero using an F-test. A new version of PRISM (2.0) was used to perform a two-way ANOVA on the data in Fig. 6 *B*.

Descriptive statistics were calculated using SYSTAT (Systat, Inc., Evanston, IL). All values are given as mean ± SEM.

### *Predicted Percent Inhibition in Fig. 6 B*

A set of predicted values for percent inhibition of total current vs voltage was derived, assuming voltage-independent inhibition of each L-current component, for a comparison with the data in Fig. 6 *B*. First, the percentages of the total tail current made up by each component (see Fig. 4 *C*) across a voltage range of −20 to +150 mV were multiplied by a single inhibition factor (reflecting voltage-independent inhibition). This factor was obtained by $(1 - y_{int})$, where $y_{int}$ was the $y$-intercept of the best-fit line in Fig. 7 *D* and represented the amount of current remaining in the presence of TRH (0.544 of the slow component and 0.778 of the fast component remain in the presence of TRH). The resulting percentage values for the fast and slow components at each voltage were summed and then subtracted from 1 to yield the predicted value for percent inhibition of the total tail current.

*Solutions and Drugs*

Stock solutions (5 mM) of racemic and specific isomers of Bay K 8644 and nimodipine were made in ethanol. TRH was kept in a stock solution (1 mM) dissolved in water. Racemic Bay K 8644 was generously donated by A. Scriabine (Miles Inc., West Haven, CT). S(−) Bay K 8644 was purchased from Research Biochemicals, Inc. (Natick, MA), and nimodipine and TRH were purchased from Sigma Chemical Co. (St. Louis, MO).

## RESULTS

### *Isolation and Characterization of L-Currents*

We began our study by recording whole-cell L-channel currents under conditions that optimized the resolution of the currents. $Ba^{2+}$ (100 mM) was used as a charge carrier, and the dihydropyridine L-channel agonist Bay K 8644 (1 μM) was used to increase the amplitude of the currents and to slow the decay of tail currents. $GH_3$ cells express both T- and L-type calcium currents (Matteson and Armstrong, 1986; Simasko et al., 1988). The L-component may be recorded in near isolation by using a holding potential of −40 mV, which inactivates T-current yet does not activate L-current (Matteson and Armstrong, 1986; Kramer et al., 1991). A representative current trace recorded under these conditions is shown in Fig. 1 *A* (trace labeled *Bay K 8644*). To confirm that this current was entirely L-current, we applied a solution that contained 1 μM of the DHP antagonist nimodipine along with 1 μM Bay K 8644. The complete block indicates that these conditions effectively isolated L-current.

To assess the voltage dependence of activation of L-channels, whole-cell $Ba^{2+}$ currents were recorded using step depolarizations from −40 mV to potentials that varied in 10-mV steps from 0 to +50 mV (absence of Bay K 8644) or −20 to +40 mV (presence of Bay K 8644). The duration of the depolarizing steps was 5 ms for currents recorded in the absence of Bay K 8644. For Bay K 8644–enhanced currents, step durations differed at each potential (e.g., 65 ms at −20 mV and 10 ms at +40 mV). Step durations were designed to be just long enough to activate L-currents fully. This protocol minimized the duration of stimulation of L-channels and was used to avoid excessive rundown and voltage-dependent inactivation. Fig. 1 *B* shows the *G–V* relationship deduced from L-channel tail currents recorded in the absence and presence of 1 μM Bay K 8644. L-currents were half-maximally activated at 13.0 ± 1.0 mV in the absence and −6.2 ± 1.0 mV in the presence of Bay K 8644. This represents a 19-mV shift in the negative direction for the voltage dependence of activation produced by Bay K 8644. In addition, Bay K 8644–modified L-currents had a steeper voltage dependence of activation than did control currents (Boltzmann slope factors were 12.1 ± 1.0 in control and 8.2 ± 0.8 in the presence of Bay K 8644). The leftward shift and increased steepness are common effects of Bay K 8644 (McDonald et al., 1994). In both the absence and presence of Bay K 8644, L-currents were maximally activated by depolarizations to +50 mV.

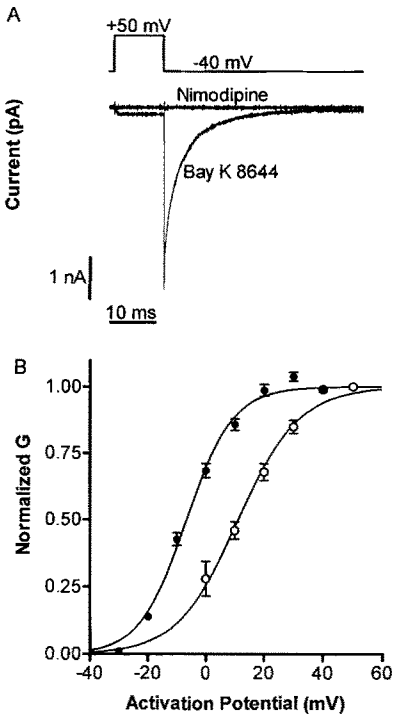


FIGURE 1. Bay K 8644–enhanced L-type $Ba^{2+}$ currents. (*A*) Representative current traces recorded in the presence of 1 μM Bay K 8644 (trace labeled *Bay K 8644*) and 1 μM Bay K 8644 + 1 μM nimodipine (trace labeled *Nimodipine*). Both traces were taken from the same cell. After recording the current in the presence of Bay K 8644, the superfusate was switched to Bay K 8644 + nimodipine. Trains of five long depolarizing pulses (+50 mV for 200 ms) were used to promote inhibition by nimodipine (a voltage-dependent inhibitor). Complete block as shown was achieved after approximately five trains. The requirement for such extensive depolarization to complete the nimodipine block was probably due to competition for the DHP receptor by the continuously present agonist, Bay K 8644. (*B*) Normalized *G* vs *V* curve deduced from tail current measurements (taken at −40 mV after step depolarizations to the potentials on the *x*-axis) in the absence (○) and presence (●) of 1 μM Bay K 8644. To calculate normalized *G*, amplitude values taken from tail peaks (absence of Bay K 8644) or exponential fits (presence of Bay K 8644) were normalized to amplitude values measured after depolarizations to +50 mV (absence of Bay K 8644) or +40 mV (presence of Bay K 8644).

### *Two Components of L-Current Deactivation*

One of the most prominent features of the Bay K 8644–enhanced L-current waveforms (Fig. 1 *A*) is the dramatically slowed tail current (McDonald et al., 1994). A kinetic analysis of this slowed tail decay is shown in Fig. 2. Representative Bay K 8644–modified tail currents recorded at −40 mV after 10-ms depolarizations to +50 mV are shown with overlaid single- (*upper traces*) and double-exponential fits (*lower traces*). Statistical analysis (see Materials and Methods) of a representative tail current indicated that the double-exponential fit was better than the single-exponential fit ($P < 0.0001$). Values for the two time constants were $\tau_{slow} = 8.4 \pm 0.3$ ms and $\tau_{fast} = 1.9 \pm 0.3$ ms ($n = 8$).

In some cell types, evidence suggestive of cooperative interactions between dihydropyridine stereoisomers of opposite action (i.e., agonist/antagonist) has been ob-

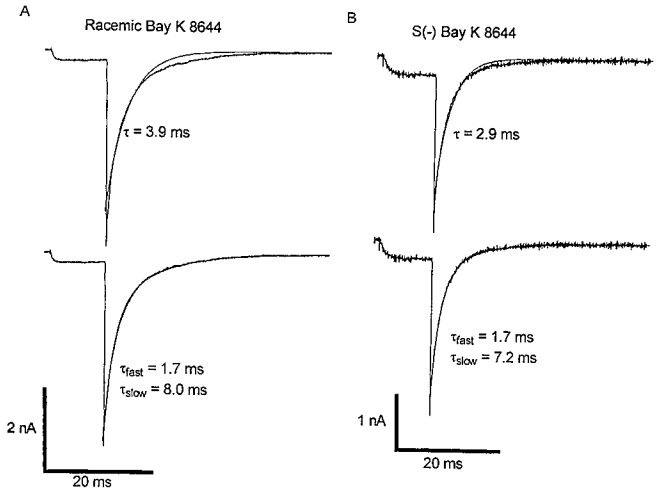


FIGURE 2. Bay K 8644–enhanced L-channel deactivation kinetics. Current traces recorded in the presence of 1 μM racemic Bay K 8644 (*A*) or 1 μM of the specific agonist enantiomer S(−)Bay K 8644 (*B*) have overlaid computer-generated single (*upper traces*) or double (*lower traces*) exponential fits.

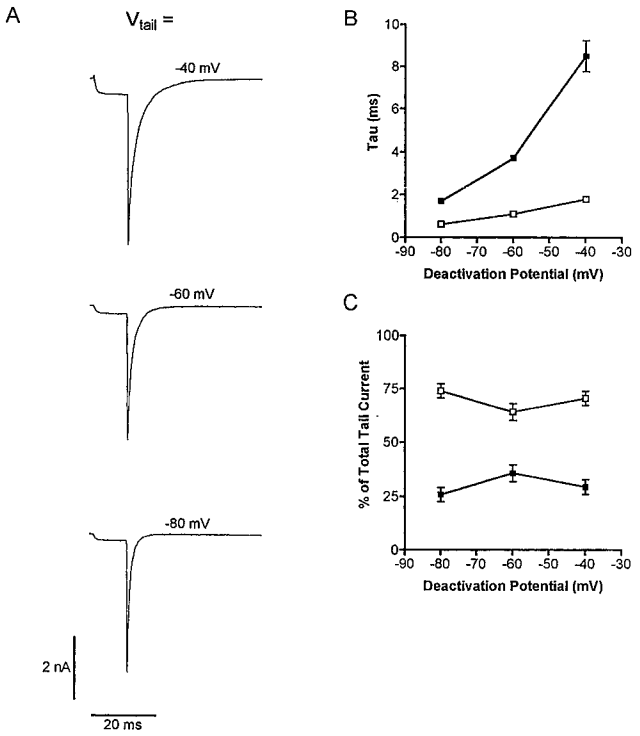


FIGURE 3. Voltage dependence of deactivation rates in the presence of 1 μM Bay K 8644. (*A*) Tail currents recorded from separate cells at deactivation potentials of −40 ($n$ = 10), −60 ($n$ = 7), and −80 mV ($n$ = 7) after 10-ms step depolarizations to +50 mV. (*B*) τ vs deactivation potential relationship for the fast (□) and slow (■) components. (*C*) Percent contribution of the fast (□) and slow (■) exponential components to the total tail current at each voltage. Percent contribution was found by dividing the amplitude of each component by the sum of the amplitudes of both components.

tained (Kokubun et al., 1986). Bay K 8644 is a racemic mixture of stereoisomers. The R(+) enantiomer is an antagonist, and the S(−) enantiomer is an agonist (Franckowiak et al., 1985). We wanted to test for any involvement of the R(+) enantiomer in producing the double-exponential tail decay. Therefore, we recorded L-channel tail currents in the presence of the specific agonist enantiomer S(−) Bay K 8644. Fig. 2 *B* shows representative current traces with overlaid single (*upper trace*) and double (*lower trace*) exponential fits. Tail current decay was again best fit ($P < 0.0001$) by two exponentials with τ's similar to those seen in racemic Bay K 8644 ($\tau_{slow}$ = 7.9 ± 0.2, $\tau_{fast}$ = 1.6 ± 0.2, $n$ = 3). Also, the percentages of the total tail current made up by each component (fast component: 71.3 ± 3.8%; slow component: 28.7 ± 3.8%) were similar to those seen in racemic Bay K 8644 (see Fig. 4 *C*). Thus, at 1 μM of drug, the double-exponential tail current decay is not a product of the interactions of the Bay K 8644 stereoisomers but, rather, reflects the actions of the specific agonist enantiomer.

The rates of tail current decay were found to depend on the repolarization potential used to measure the tail. Fig. 3 *A* shows representative current traces elicited in the presence of 1 μM Bay K 8644 by 10-ms depolarizations to +50 mV followed by 40-ms repolarizations to −40, −60, and −80 mV. Tails at all three potentials were fit by two exponentials. The τ vs repolarization voltage relationship is shown in Fig. 3 *B*. Both τ's increase approximately twofold for each 20 mV of depolarization in the voltage range shown in the figure. Fig. 3 *C* shows that the percentages of the total tail current accounted for by each component do not change with changes in the repolarization potential ($P$ = 0.77).

### *The Two Components Differ in Voltage Dependence of Activation*

Tail currents with two exponential components shown in Figs. 1–3 were recorded after depolarizations to a potential (+50 mV) that maximally activates L-currents. We wished to measure activation of the two tail components at lower levels of depolarization. Therefore, we analyzed deactivation of L-currents activated by a range of depolarizations. We found that the two exponential components had distinct voltage dependences of activation. Fig. 4 *A* shows $G$–$V$ plots (with overlaid Boltzmann fits) constructed for each component. The voltage dependence of activation of the slow tail current component was shifted to the left by ~16 mV relative to the fast component (Fig. 4 *A*; $V_{0.5slow}$ = −15.3 ± 1.4 mV and $V_{0.5fast}$ = 1.2 ± 0.9 mV, $n$ = 8). The steepness of the voltage dependence of activation (SLOPE in the Boltzmann equation) was 6.3 ± 1.4 mV for the slow component and 8.0 ± 0.8 mV for the fast component. The 95% confidence intervals for the two slope factors overlap, indicating that they are not statistically different. The time constants of tail current decay were indepen-

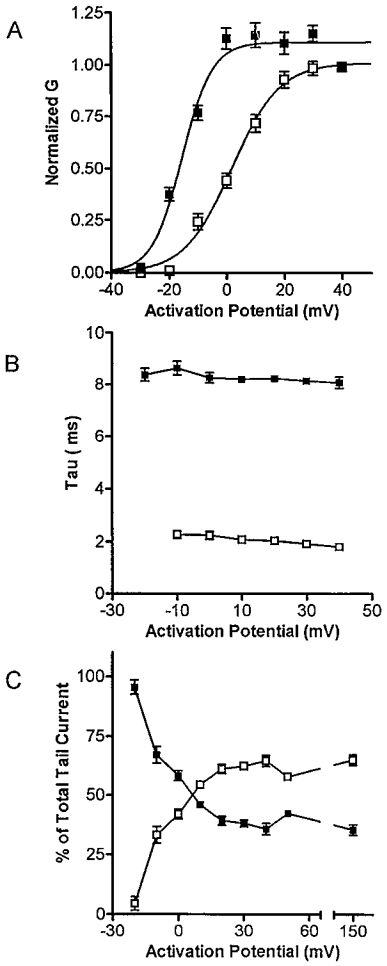


FIGURE 4. Voltage dependence of activation of the two Bay K 8644–revealed tail current components and their relative contributions to the total tail current. (*A*) Normalized *G–V* relationships (with overlaid smooth curve Boltzmann equation fits) for the fast (□) and slow (■) components. Normalization to amplitude values at +40 mV produced normalized *G*. $V_{0.5slow} = -15.5 \pm 1.4$ mV, $V_{0.5fast} = 1.8 \pm 1.1$ mV, $n = 9$. (*B*) Time constants of deactivation of the fast (□) and slow (■) components are independent of the potential of the step depolarizations used to activate L-currents (tails were always measured at −40 mV). (*C*) The percent contribution of the fast (□) and slow (■) components to the total tail current (measured at −40 mV) is plotted as a function of the voltage of the step depolarization used to activate L-currents.

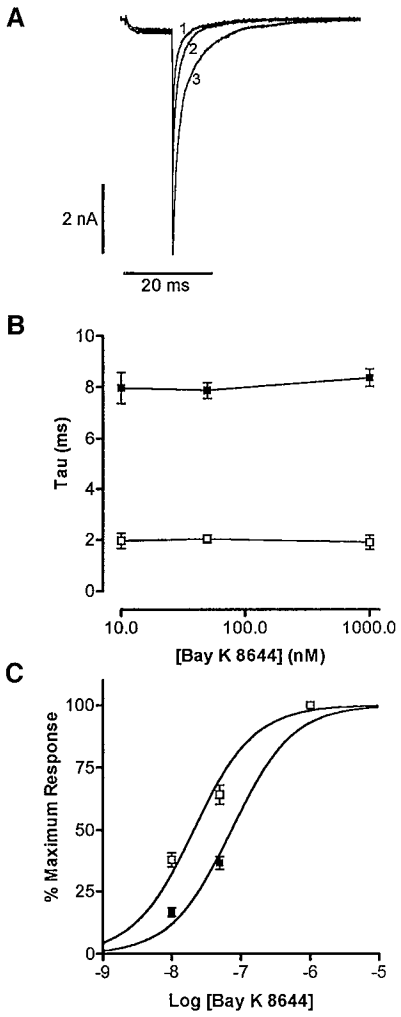


FIGURE 5. Bay K 8644 sensitivities of the two tail current components. (*A*) Representative currents recorded in the presence of three concentrations (1 = 10 nM, 2 = 50 nM, 3 = 1 μM) of Bay K 8644. The holding and repolarization potential was −40 mV, and the depolarization was to +50 mV for 10 ms. (*B*) Time constants of deactivation of the fast (□) and slow (■) components are independent of [Bay K 8644]. (*C*) Dose–response relationship for each of the fast (□) and slow (■) tail current components. For each experiment, amplitude values for each component were normalized to amplitudes at 1 μM Bay K 8644. Computer-generated sigmoidal dose–response functions (smooth curves—see Materials and Methods) gave the values $EC_{50slow} = 73.6$ nM, $EC_{50fast} = 21.0$ nM.

dent of the potential of the depolarizing step (Fig. 4 *B*). Thus, the slow component is activated at more negative potentials than the fast component, and the degree of activation of the components has no effect on their deactivation rates.

Because the two components are activated to different degrees at any given submaximal level of depolarization, their relative contribution to the total tail current will differ across test voltages. These relative contributions to total tail current are shown in Fig. 4 *C*. Each data point was found by dividing the amplitude of each component by the total tail current amplitude (recorded at −40 mV) after a depolarization to the potential on the *x*-axis. At −20 mV, the tail is virtually entirely slow component—in six out of eight cells, no fast component was detectable at −20 mV. When both components are maximally activated (i.e., $>\sim+40$ mV), the fast component accounts for 62% of the tail and the slow component accounts for 38% (values are means of data points at +40, +50, and +150 mV in Fig. 4 *D*). Thus, whereas the fast component accounts for the majority of the total activatable L-current, small depolarizations will activate mostly the slow component of L-current.

### *The Two Components Differ in Their Sensitivities to Bay K 8644*

We also attempted to determine the sensitivity of each tail current component to racemic Bay K 8644. A simple dose–response experiment was performed in which three concentrations (in order of application: 10 nM, 50 nM, and 1 μM) of Bay K 8644 were applied while recording whole-cell $Ba^{2+}$ tail currents. [Bay K 8644] was increased to a new level only after currents had reached maximal enhancement at the previous concentration. Representative currents are shown in Fig. 5 *A*. When subsaturating concentrations were applied, tail current decay at −40 mV could be fit by three exponentials: $\tau = \sim150$ μs for unmodified L-channels (consistent with Matteson and Armstrong, 1986), and $\tau = \sim2$ and $\sim8$ ms for the fast and slow components of Bay K 8644-modified L-channels, respectively. The fastest compo-

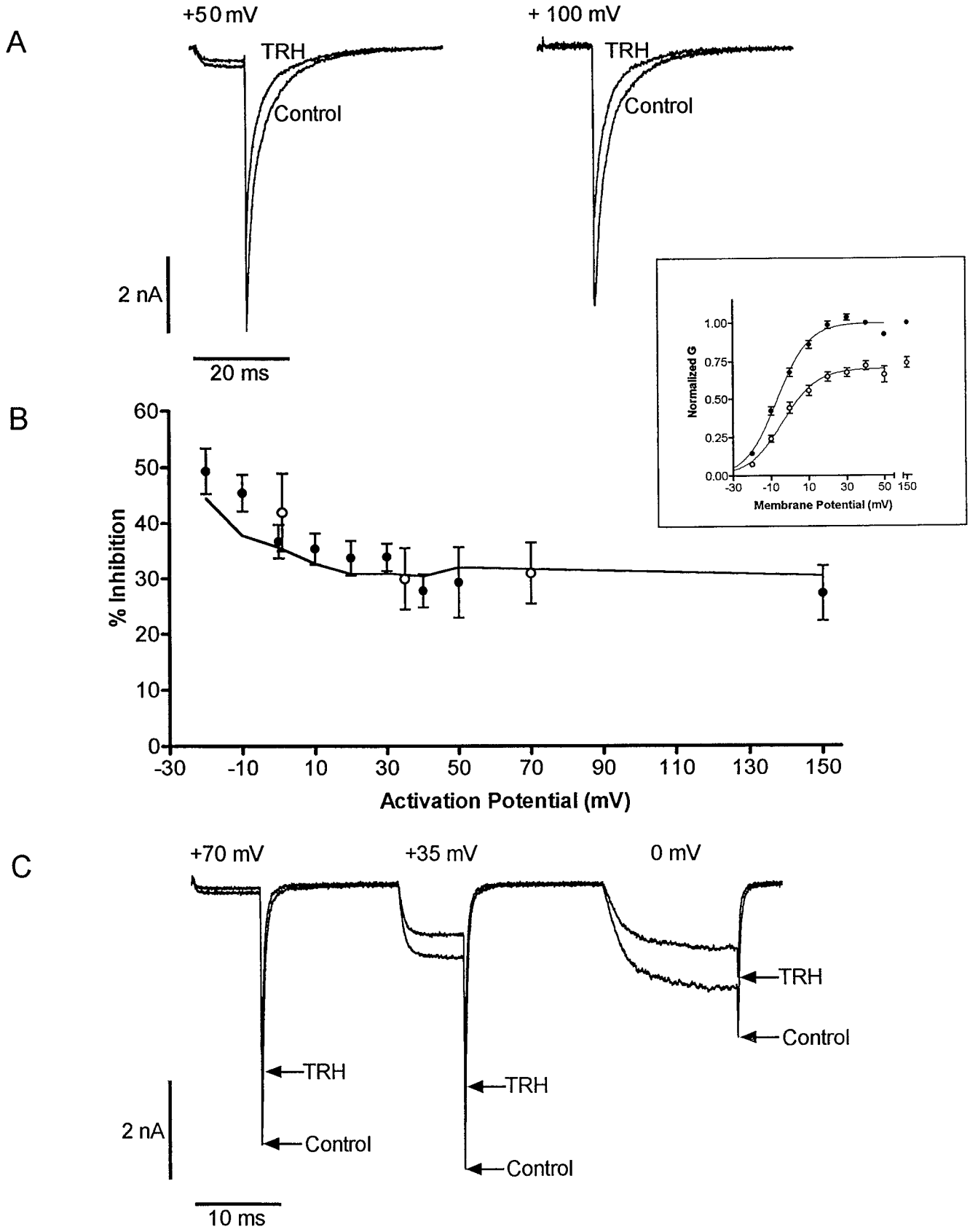
A
+50 mV
TRH
Control
+ 100 mV
TRH
Control
2 nA
20 ms
Normalized G
1.00
0.75
0.50
0.25
0.00
-30
-10
10
30
50
150
Membrane Potential (mV)
B
% Inhibition
60
50
40
30
20
10
0
-30
-10
10
30
50
70
90
110
130
150
Activation Potential (mV)
C
+70 mV
+35 mV
0 mV
TRH
Control
TRH
Control
TRH
Control
2 nA
10 ms

nent was not observed in the presence of 1 μM Bay K 8644, consistent with this being a saturating concentration. Fig. 5 *B* shows that the time constants of each Bay K 8644–revealed component of tail current decay did not depend on [Bay K 8644]. Dose–response relations for each component derived from the amplitudes of each component normalized to their amplitudes at 1 μM Bay K 8644 are plotted in Fig. 5 *C*. Current rundown prevented the application of more than three concentrations of Bay K 8644, and, hence, full dose–response curves could not be constructed. Nevertheless, $EC_{50}$ values indicate that the fast component is more sensitive to racemic Bay K 8644 than the slow component ($EC_{50fast}$ = ~21 nM, $EC_{50slow}$ = ~74 nM).

*Tail Current Analysis of TRH-induced Inhibition of L-Current*

TRH inhibits L-type calcium currents in $GH_3$ cells (Levitan and Kramer, 1990; Gollasch et al., 1991; Simasko, 1991) by releasing $Ca^{2+}$ from intracellular stores (Kramer et al., 1991). We wished to perform a detailed analysis of this inhibition. Specifically, we were interested in comparing the effects of TRH on each Bay K 8644–revealed component of L-current. In addition, we wanted to test whether the degree of inhibition varied with the potential used to activate the L-currents, as has been observed in several cases of N-type $Ca^{2+}$ current modulation (e.g., Bean, 1989*b*). Therefore, we recorded tail currents in the absence and presence of TRH after depolarizations to a variety of potentials. To minimize the amount of stimulation (and subsequent rundown) of a given cell's $Ca^{2+}$ channels, three variations of experiment were performed on separate cells, and all data were combined for analysis. General trends in the data did not vary across experimental variations. In the first experiment ($n$ = 3), cells were depolarized to −10, +10, +30, +50, +100, and +150 mV. In the second experiment ($n$ = 6), cells were depolarized over the range of −20 to +40 mV in 10-mV increments. In the third experiment ($n$ = 2), cells were depolarized over the range of +40 to −20 mV in −10-mV increments (i.e., in reverse order to control for an order effect). In all experiments, the depolarizations were just long enough to activate L-currents fully, and repolarizations for measurements of tail currents were always to −40 mV. Analysis of tail currents was performed as described above (i.e., by exponential curve fitting).

Representative currents recorded in the absence and presence of TRH at +50 and +150 mV are shown in Fig. 6 *A*. The inset in Fig. 6 shows the $G$ vs $V$ for total Bay K 8644–modified L-currents in the absence and presence of TRH. Both Fig. 6 *A* and the inset show that inhibition of tail currents is evident even after strong depolarizations. The percent inhibition vs voltage relationship for total L-currents (Fig. 6 *B*) indicates that percent inhibition decreases between −20 and +40 mV but then settles at a plateau level that is maintained at higher voltages.

The magnitude of TRH inhibition of $GH_3$ cell L-currents evoked by a depolarization to 0 mV was found to be the same both in the absence and presence of Bay K 8644 (Kramer et al., 1991). To extend this comparison further, we tested the voltage dependence of TRH inhibition in the absence of Bay K 8644. Tail currents were measured at −40 mV after depolarizations to three potentials (0, +35, and +70 mV). Fig. 6 *C* shows representative currents evoked by depolarizations to these three potentials in the absence and presence of 1 μM TRH. Data points for the mean percent inhibition of peak tail current at each voltage for recordings made in the absence of Bay K 8644 ($n$ = 4) are shown as open circles in Fig. 6 *B*. The data obtained in the absence and presence of Bay K 8644 are similar: First, inhibition is evident even after strong depolarizations; second, percent inhibition is greatest at lower levels of depolarization (e.g., 0 mV) and decreases to a plateau level at more positive potentials. These two observations suggested that TRH inhibition might involve a mixture of voltage-dependent and voltage-independent processes. To clarify the nature of TRH inhibition of Bay K 8644–modified L-currents, we analyzed the effect of TRH on each component.

*The Two Components Differ in Their Sensitivities to Inhibition by TRH*

In addition to their differences in voltage dependence of activation and sensitivity to Bay K 8644, we found that the two tail current components differed in the de-

FIGURE 6. Voltage dependence of TRH inhibition in the absence and presence of 1 μM Bay K 8644. (*A*) Representative Bay K 8644–enhanced current traces recorded in the absence and presence of 1 μM TRH. Tails were recorded upon repolarization to −40 mV after 10-ms depolarizations to the indicated potentials. (*B*) Percent inhibition vs voltage plot for total tail currents in the absence (○) and presence (●) of Bay K 8644. For data obtained in the absence of Bay K 8644, amplitude values were from measurements of the tail current at its peak. The line connects predicted percent inhibition values, which were derived assuming voltage-independent inhibition (see Materials and Methods). (*C*) Representative Bay K 8644–free current traces recorded in the absence and presence of 1 μM TRH. From a holding potential of −40 mV, cells were depolarized for 7.5, 7.5, and 15 ms to +70, +35, and 0 mV, respectively. Tails were recorded during 15-ms repolarizations to −40 mV after each depolarization. The triple pulse was given at a rate of 0.2 Hz. (*Inset*) Normalized $G$ vs membrane potential for total Bay K 8644–modified L-currents in the absence (●) and presence (○) of 1 μM TRH. Amplitude values were obtained as the sum of the two amplitudes from double-exponential fits of tail currents recorded at −40 mV after depolarizations across a range of potentials and then normalized to the amplitude value at +40 mV ($n$ = 7; data encompassed by Boltzmann fits) or +150 mV ($n$ = 3; data at +50 and +150 mV) in the absence of TRH. The smooth curves are fits of the data to a Boltzmann equation.

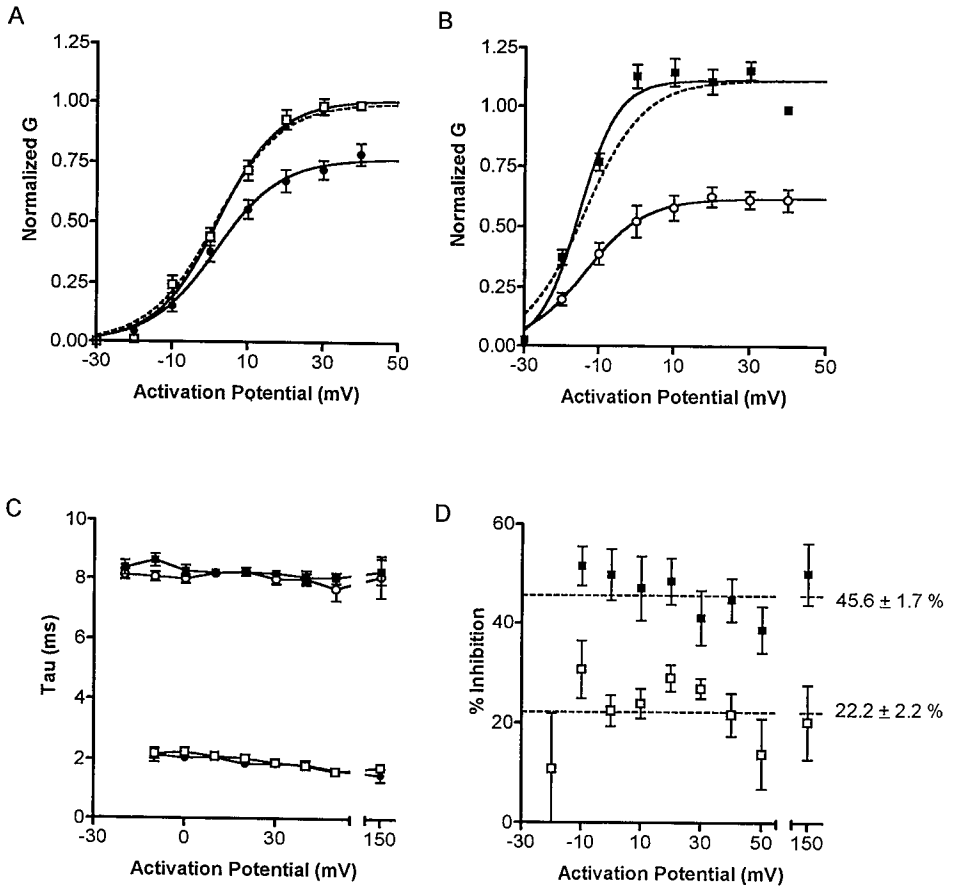


FIGURE 7. TRH inhibition of Bay K 8644–modified L-currents components. (*A*) Normalized *G–V* relationship for the fast component in the absence (□) and presence (●) of 1 μM TRH. (*B*) Normalized *G–V* relationship for the slow component in the absence (■) and presence (○) of 1 μM TRH. In *A* and *B*, all values are normalized to the amplitude of control current components at +40 mV. See text for V50 and SLOPE values for Boltzmann fits (smooth curve) to each plot. The dashed lines are scaled-up versions of the Boltzmann equation fits of the normalized *G* values for current components recorded in the presence of TRH. (*C*) TRH does not affect the rates of tail current decay. At all levels of depolarization, tail τ's for the fast and slow components were not changed by TRH (□, fast component, absence of TRH; ○, fast component, presence of TRH; ■, slow component, absence of TRH; ○, slow component, presence of TRH). (*D*) Percent inhibition vs voltage plot for the fast (□) and slow (■) components of the tail. Ratios of amplitude values for each component in the presence and absence of TRH are plotted for each voltage. A least-squares best-fit line (*dashed line*) with a slope of zero is laid over the data for each component. The average percent inhibition of each component is shown to the right of each fit.

gree to which they were inhibited by TRH. *G–V* plots for the two tail current components in the absence and presence of TRH are shown in Fig. 7, *A* and *B*. A comparison of the two plots reveals that the slow component is inhibited to a greater degree than the fast component. The time constants of each component of tail current decay (Fig. 7 *C*) were not changed by TRH. Fig. 7 *D* shows the percent inhibition vs voltage relationships for the two components of the tail current. TRH inhibited both the slow and the fast component after depolarizations to all potentials, and the slow component was consistently inhibited to a greater degree than the fast component (mean inhibition was 46% for the slow component vs 22% for the fast component). Thus, the slow component is more sensitive to 1 μM TRH.

### *Voltage Independence of TRH Inhibition of Each Component*

It has been observed that the degree of inhibition of $Ca^{2+}$ channel currents by certain neuromodulatory substances can change with the level of depolarization used to evoke the current (Bean, 1989*b*). In Fig. 7 *D*, the percent inhibition for each component shows only a mild decline over a 170-mV range of test potentials. In fact, linear regression fits of data points for each component give slopes that are not significantly different from 0 ($P > 0.05$ in both cases). In contrast, percent inhibition falls sharply to 0 over a similar voltage range in a case where neurotransmitter-induced inhibition was found to be voltage dependent (see Fig. 1 *C* in Bean, 1989*b*). Thus, the relative flatness of the percent inhibition vs voltage relationship for each tail current component indicates voltage-independent inhibition of both components. Hence, we conclude that both components are inhibited in a voltage-independent manner. We propose that the voltage dependence of inhibition of the total tail current at potentials between −20 and 0 mV (Fig. 6 *B*) is due to the different voltage dependences of activation of the two tail current components. To test this idea, we produced a set of predicted percent inhibition values for total tail currents over the voltage range of the data in Fig. 6 *B*, assuming voltage-independent inhibition of each component (see Materials and Methods). These predicted percent inhibition values are connected by the continuous line in Fig. 6 *B*, which is laid over the observed data points. This line matches the shape of the observed data. The deviation of the line from the data near −20 mV arises

from the fact that the inhibition factors used to produce the predicted values (see Materials and Methods) are the best-fit middle of the data in Fig. 7 *D*. These data differ overall by ~10% across the total voltage range. Moreover, a comparison of the predicted values with the observed data obtained in the presence of Bay K 8644 across all voltages yielded no significant differences (two-way ANOVA; $P$ values were $> 0.05$). Thus, the reproduction of the general shape of the data by the predicted values line further suggests that inhibition of each component by TRH is voltage independent.

The voltage-independent nature of TRH inhibition of each component of Bay K 8644–enhanced current suggested that the voltage dependence of activation of the two tail components would not be affected by TRH. From Fig. 7, *A* and *B*, the half-maximal activation voltages and slope factors were in control: $V_{0.5slow} = -15.5$ mV, $slope_{slow} = 5.3$, $V_{0.5fast} = 1.8$ mV, $slope_{fast} = 8.2$; and in the presence of TRH: $V_{0.5slow} = -14.1$ mV, $slope_{slow} = 8.1$, $V_{0.5fast} = 1.3$ mV, $slope_{fast} = 8.7$. The 95% confidence intervals for each of these pairs of means overlap, indicating that they are not statistically different. As expected from these statistical results, the Boltzmann equation fits of data obtained in the presence of TRH scale up to meet the control data (Fig. 7, *A* and *B*, *dashed lines*) reasonably well (the discrepancy between the scaled up fit and the data in Fig. 7 *B* is due to the lack of a data point at −30 mV in the presence of TRH).

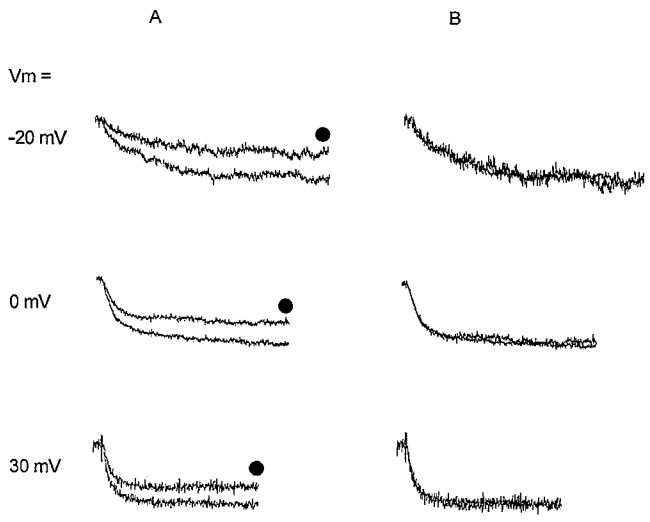


FIGURE 8. TRH does not alter L-current activation kinetics. (*A*) Waveforms representing Bay K 8644–modified current activation in the absence (●) and presence of 1 μM TRH recorded at the potentials indicated beside each trace. Time and current scales differ for each trace and are not shown. Depolarizations were for 65 ms (at −20 mV), 45 ms (at 0 mV), and 20 ms (at 30 mV). (*B*) Superimposition of traces in *A*, produced by scaling up the trace recorded in the presence of TRH. The close correspondence of control and TRH traces indicates that TRH does not alter activation kinetics.

Hence, TRH does not alter the voltage dependence of activation of either component.

Voltage-dependent inhibition of $Ca^{2+}$ channels is often associated with a slowing of activation kinetics (Marchetti et al., 1986; Elmslie et al., 1990). Fig. 8 *A* shows representative current traces recorded during step depolarizations to three potentials in the absence and presence of 1 μM TRH. In Fig. 8 *B*, the traces recorded in the presence of TRH have been scaled up to match the size of the control traces. From the close superimposition of the overlaid control and TRH traces, it is apparent that activation kinetics are not altered by TRH.

## DISCUSSION

### *DHP Agonist Bay K 8644 Reveals Two Components of L-Type $Ca^{2+}$ Channel Current in $GH_3$ Cells*

Tail current analysis has been used to identify two voltage-gated $Ca^{2+}$ currents in $GH_3$ cells (Matteson and Armstrong, 1986). Subsequent work revealed that these currents can be identified as DHP-sensitive (L) and DHP-insensitive (T) currents (Simasko et al., 1988). In this report, we use the analysis of tail currents recorded in the presence of the DHP agonist Bay K 8644 to reveal two components of DHP-sensitive L-current in $GH_3$ cells. The two components have different functional properties (summarized in Table I). In the presence of Bay K 8644, the two components have distinct deactivation kinetics (Fig. 2). The two components also differ in their voltage dependence of activation (Fig. 4), in their sensitivity to racemic Bay K 8644 (Fig. 5), and in the degree to which they are inhibited by TRH (Fig. 7).

### *Biexponential Deactivation of L-Channel Current*

In the absence of DHP agonists, whole-cell L-type $Ca^{2+}$ channel currents in $GH_3$ cells are small in size, are half-maximally activated at +13 mV (Fig. 1 *B*), and show extremely rapid deactivation kinetics (Matteson and Armstrong, 1986). The extreme rapidity of tail current decay hinders an accurate kinetic analysis of deactivation. In the presence of Bay K 8644, L-type $Ca^{2+}$ channel currents in $GH_3$ cells are altered in the following ways: Current amplitude is increased, the half-maximal activation voltage is shifted leftward, and deactivation is

TABLE I

*Summary of the Functional Characteristics of the Two L-Current Components in $GH_3$ Cells*

| Component | Decay τ at −40 mV | $V_{0.5}$ | Bay K 8644 $EC_{50}$ | Percent inhibition by 1 μM TRH | Percent total current |
|---|---|---|---|---|---|
| Fast | ~2 ms | ~1 mV | ~21 nM | ~22 | ~62 |
| Slow | ~8 ms | ~−15 mV | ~74 nM | ~46 | ~38 |

slowed dramatically. The slowed tails have a double exponential decay (Fig. 2). There is precedence for each of these effects from previous studies (for review see McDonald et al., 1994) with the exception of the double-exponential nature of the slowed tail decay. Previous studies that report exponential fits of DHP-slowed tail currents (Droogmans and Callewaert, 1986; Marks and Jones, 1992; Bechem and Hoffmann, 1993; Zidanic and Fuchs, 1995) have shown that one exponential produces an adequate fit (with one significant exception—Lacerda and Brown, 1989—see below). Thus, we feel that it is most likely that the Bay K 8644–revealed double exponential L-channel tail current decay reflects complexity in $GH_3$ L-channel properties rather than a previously unknown characteristic of DHP agonist modulation.

In a study of L-channels in cardiac myocytes, Lacerda and Brown (1989) found that two exponentials were required to produce an adequate fit of tail currents recorded in the presence of Bay K 8644. Thus, myocyte L-channels appear similar to $GH_3$ L-channels in Bay K 8644–modified deactivation properties. However, Lacerda and Brown also found DHP agonist concentration-dependent changes in L-current tail decay time constants. Our data in Fig. 5 *B* are in direct contrast with this finding. We observed no such concentration-dependent changes in tail decay time constants. Rather, the amplitudes of each of our exponential components were increased as [Bay K 8644] increased. Their analysis protocol involved fitting their L-channel tail currents to the same number of exponentials (two) both in the absence and presence of Bay K 8644. In contrast, we fit tails recorded in the absence of Bay K 8644 with a single-exponential equation, and then we added exponential components (two) to the equation used to fit our L-channel tail currents recorded in the presence of Bay K 8644. Thus, tail currents recorded in the presence of Bay K 8644 were fit by three exponentials (except at 1 μM Bay K 8644, where we used an equation with only the slower two exponentials since the fastest component was not present). If we had fit our Bay K 8644–slowed tail currents with a single-exponential equation, we would have produced data indicating concentration-dependent changes in the rate of deactivation. Thus, the contrast between our dose–response findings and those of Lacerda and Brown (1989) may be due to the differences in our analysis protocols. Alternatively, the mechanisms of DHP agonist modulation of L-channels may differ across cell types.

### *TRH-induced Inhibition of Each Component Is Voltage Independent*

There have been numerous reports of TRH inhibition of L-currents in $GH_3$ cells (Levitan and Kramer, 1990; Gollasch et al., 1991; Kramer et al., 1991). In the present study, we examined the voltage dependence of this inhibition. In other cell types, studies of voltage-dependent inhibition show the following: (*a*) Macroscopic $Ca^{2+}$ currents (when analyzed without separation into components) are reduced in magnitude relative to control after small depolarizations, but not after strong depolarizations (e.g., Bean, 1989*b*). (*b*) The voltage dependence of activation of $Ca^{2+}$ currents is shifted to more positive potentials (Bean, 1989). (*c*) $Ca^{2+}$ current activation kinetics may be slowed (e.g., Marchetti et al., 1986; Elmslie et al., 1990). (*d*) Strong depolarization can transiently reverse the inhibitory effects (e.g., Marchetti et al., 1986; Elmslie et al., 1990). In contrast with these characteristic observations of voltage-dependent inhibition, we have found that TRH inhibition of $GH_3$ L-currents is still evident (not detectably reversed) after strong depolarizations (trace labeled +150 mV in Fig. 6 *A*), that TRH does not alter the voltage dependence of activation of L-currents (Fig. 7), and that TRH does not alter L-current activation kinetics (Fig. 8). Furthermore, percent inhibition of each component of L-current does not vary significantly with voltage (Fig. 7). These findings suggest that TRH inhibition is voltage independent.

Therefore, the apparent mixture of voltage-dependent and -independent inhibitory mechanisms implied by the complex percent inhibition vs voltage relationship for total L-currents recorded in the presence of Bay K 8644 (Fig. 6 *B*, *solid circles*) may be explained by the varying relative contributions of each component to the total tail current across voltages (Fig. 4 *C*). These varying relative contributions are due to the different voltage dependences of activation of each component (Fig. 4 *A*). This explanation is affirmed by the approximation of the shape of the raw data by the predicted percent inhibition values line in Fig. 6 *B*, which was derived based on the assumption of voltage-independent inhibition of each component (see Materials and Methods). The data obtained in the absence of Bay K 8644 (Fig. 6 *B*, *open circles*) also fall along this predicted inhibition line, and, thus, unmodified L-currents may consist of two components with different voltage dependences of activation. Unfortunately, detection of two exponential components in tail currents recorded in the absence of Bay K 8644 would likely require presently unattainable (μs) whole-cell voltage-clamp speeds. However, our data in the presence of Bay K 8644 indicate that the molecular mechanism of TRH inhibition of each component should be considered to be voltage independent. Note that this explanation of apparent mixed voltage-dependent and -independent inhibition invokes a single signal transduction mechanism, in contrast with other explanations that invoke multiple signal transduction mechanisms (Hille et al., 1995).

We thank Dr. J. Johnson for helpful comments on the manuscript.

Funding for this study was provided by a grant-in-aid from the American Heart Association (Pennsylvania affiliate), a Klingenstein Fellowship in the Neurosciences, and National Institutes of Health grants NS29804 and NS32385 to E.S. Levitan. D.M. Fass was supported by a National Institute of Mental Health training grant (MH18273). E.S. Levitan is an Established Investigator of the American Heart Association.

*Original version received 8 December 1995 and accepted version received 3 April 1996.*

## REFERENCES

Bean, B.P. 1989*a*. Classes of calcium channels in vertebrate cells. *Annu. Rev. Physiol.* 51:367–384.

Bean, B.P. 1989*b*. Neurotransmitter inhibition of neuronal calcium currents by changes in channel voltage dependence. *Nature (Lond.).* 340:153–156.

Bechem, M., and M. Hoffmann. 1993. The molecular mode of action of the Ca agonist (−) Bay K 8644 on the cardiac Ca channel. *Pflüg. Arch. Eur. J. Physiol.* 424:343–353.

Cognard, C., M. Lazdunski, and G. Romey. 1986. Different types of $Ca^{2+}$ channels in mammalian skeletal muscle cells in culture. Proc. Natl. Acad. Sci. USA. 83:517–521.

Delcour, A.H., and R.W. Tsien. 1993. Altered prevalence of gating modes in neurotransmitter inhibition of N-type calcium channels. *Science (Wash. DC).* 259:980–984.

Droogmans, G., and G. Callewaert. 1986. $Ca^{2+}$-channel current and its modification by the dihydropyridine agonist Bay k 8644 in isolated smooth muscle cells. *Pflüg. Arch. Eur. J. Physiol.* 406:259–265.

Elmslie, K.S., W. Zhou, and S.W. Jones. 1990. LHRH and GTP-γ-S modify calcium current activation in bullfrog sympathetic neurons. *Neuron.* 5:75–80.

Franckowiak, G., M. Bechem, M. Schramm, and G. Thomas. 1985. The optical isomers of the 1,4-dihydropyridine Bay K 8644 show opposite effects on $Ca^{2+}$ channels. *Eur. J. Pharmacol.* 114:223–226.

Gollasch, M., H. Haller, G. Schultz, and J. Hescheler. 1991. Thyrotropin-releasing hormone induces opposite effects on $Ca^{2+}$ channel currents in pituitary cells by two pathways. *Proc. Natl. Acad. Sci. USA.* 88:10262–10266.

Hamill, O.P., A. Marty, E. Neher, B. Sakmann, and F.J. Sigworth. 1981. Improved patch-clamp techniques for high-resolution current recording from cells and cell-free membrane patches. *Pflüg. Arch. Eur. J. Physiol.* 391:85–100.

Hess, P. 1990. Calcium channels in vertebrate cells. *Annu. Rev. Neurosci.* 13:337–356.

Hille, B., D.J. Beech, L. Bernheim, A. Mathie, M.S. Shapiro, and L.P. Wollmuth. 1995. Multiple G-protein-coupled pathways inhibit N-type Ca channels of neurons. *Life Sci.* 56:989–992.

Kokubun, S., B. Prod'hom, C. Becker, H. Porzig, and H. Reuter. 1986. Studies on Ca channels in intact cardiac cells: voltage-dependent effects and cooperative interactions of dihydropyridine enantiomers. *Mol. Pharmacol.* 30:571–584.

Kramer, R.H., L.K. Kaczmarek, and E.S. Levitan. 1991. Neuropeptide inhibition of voltage-gated calcium channels mediated by mobilization of intracellular calcium. *Neuron.* 6:557–563.

Lacerda, A.E., and A.M. Brown. 1989. Nonmodal gating of cardiac calcium channels as revealed by dihydropyridines. *J. Gen. Physiol.* 93:1243–1273.

Levitan, E.S., and R.H. Kramer. 1990. Neuropeptide modulation of single calcium and potassium channels detected with a new patch clamp configuration. *Nature (Lond.).* 348:545–547.

Lievano, A., A. Bolden, and R. Horn. 1994. Calcium channels in excitable cells: divergent genotypic and phenotypic expression of $\alpha_1$-subunits. *Am. J. Physiol.* 267:C411–C424.

Marchetti, C., E. Carbone, and H.D. Lux. 1986. Effects of dopamine and noradrenaline on Ca channels of cultured sensory and sympathetic neurons of chick. *Pflüg. Arch. Eur. J. Physiol.* 406:104–111.

Marks, T.N., and S.W. Jones. 1992. Calcium currents in the A7r5 smooth muscle-derived cell line. *J. Gen. Physiol.* 99:367–390.

Matteson, D.R., and C.M. Armstrong. 1986. Properties of two types of calcium channels in clonal pituitary cells. *J. Gen. Physiol.* 87: 161–182.

McDonald, T.F., S. Pelzer, W. Trautwein, and D.J. Pelzer. 1994. Regulation and modulation of calcium channels in cardiac, skeletal, and smooth muscle cells. *Physiol. Rev.* 74:365–507.

Neveu, D., J. Nargeot, and S. Richard. 1993. Two high-voltage-activated, dihydropyridine-sensitive $Ca^{2+}$ channel currents with distinct electrophysiological and pharmacological properties in cultured rat aortic myocytes. *Pflüg. Arch. Eur. J. Physiol.* 424:45–53.

Neveu, D., J.F. Quignard, A. Fernandez, S. Richard, and J. Nargeot. 1994. Differential β-adrenergic regulation and phenotypic modulation of voltage-gated calcium currents in rat aortic myocytes. *J. Physiol. (Camb.).* 479:171–182.

Richard, S., F. Tiaho, P. Charnet, J. Nargeot, and J.M. Nerbonne. 1990. Two pathways for $Ca^{2+}$ channel gating differentially modulated by physiological stimuli. *Am. J. Physiol.* 258:H1872–H1881.

Simasko, S.M., G.A. Weiland, and R.E. Oswald. 1988. Pharmacological characterization of two calcium currents in $GH_3$ cells. *Am. J. Physiol.* 254:E328–E336.

Simasko, S.M. 1991. Reevaluation of the electrophysiological actions of thyrotropin-releasing hormone in a rat pituitary cell line ($GH_3$). *Endocrinology.* 128:2015–2026.

Tanabe, T., B.A. Adams, S. Numa, and K.G. Beam. 1991. Repeat I of the dihydropyridine receptor is critical in determining calcium channel activation kinetics. *Nature (Lond.).* 352:800–803.

Tiaho, F., S. Richard, P. Lory, J.M. Nerbonne, and J. Nargeot. 1990. Cyclic-AMP-dependent phosphorylation modulates the stereospecific activation of cardiac Ca channels by Bay K 8644. *Pflüg. Arch. Eur. J. Physiol.* 417:58–66.

Worley, J.F., J.W. Deitmer, and M.T. Nelson. 1986. Single nisoldipine-sensitive calcium channels in smooth muscle cells isolated from rat mesenteric artery. *Proc. Natl. Acad. Sci. USA.* 83:5746–5750.

Yue, D.T., S. Herzig, and E. Marban. 1990. β-adrenergic stimulation of calcium channels occurs by potentiation of high-activity gating modes. *Proc. Natl. Acad. Sci. USA.* 87:753–757.

Zidanic, M., and P.A. Fuchs. 1995. Kinetic analysis of barium currents in chick cochlear hair cells. *Biophys. J.* 68:1323–1336.